

A Retroviral Wild-type *p53* Expression Vector Penetrates Human Lung Cancer Spheroids and Inhibits Growth by Inducing Apoptosis¹

Toshiyoshi Fujiwara, Elizabeth A. Grimm, Tapas Mukhopadhyay, De Wei Cai, Laurie B. Owen-Schaub, and Jack A. Roth²

The Departments of Thoracic and Cardiovascular Surgery [T. F., T. M., D. W. C., J. A. R.], Tumor Biology [E. A. G., J. A. R.], General Surgery [E. A. G.], and Immunology [L. B. O.-S.], The University of Texas M. D. Anderson Cancer Center, Houston, Texas 77030

Abstract

Multicellular tumor spheroids approximate the three-dimensional configuration of primary and metastatic tumors. The effects of retrovirus-mediated transduction of wild-type *p53* (wt-*p53*) were studied on multicellular tumor spheroids of human non-small cell lung cancer cell lines H322a, the *p53* gene of which is homozygously mutated at codon 248, and WT226b, which has endogenous wt-*p53*. The growth of WT226b spheroids was not affected by exogenous wt-*p53* transduction; the growth of H322a spheroids, however, was significantly inhibited by the addition of wt-*p53* virus stocks. Transduction of cells by the wt-*p53* retroviral vector and penetration of multiple cell layers in H322a spheroids was demonstrated by *in situ* polymerase chain reaction/hybridization with the neomycin-resistant *neo* probe. Apoptotic changes indicating programmed cell death were observed in H322a spheroids treated with the wt-*p53* virus. These results suggest that retroviral vectors can penetrate into multiple cell layers of three-dimensional tumor masses and induce potentially therapeutic effects.

Introduction

Recombinant retroviruses are widely used as vectors for the transfer of exogenous genes into mammalian cells (1). The construction of safe amphotropic packaging cell lines that produce high-titer helper-free retroviruses has facilitated application of this system in human gene therapy (2). Protocols for the transduction of cytokine genes into lymphocytes and tumor cells to enhance activation of the cytotoxic immune response against malignant tumors are under clinical investigation (3). Direct modulation of oncogene and tumor suppressor gene expression using local delivery of viral vectors has recently been proposed (4).

Recent advances in molecular genetics have shown that the development of human cancer is the result of several genetic alterations and that loss of the genome-guarding function of the *p53* gene is one of the most common events in tumorigenesis (5, 6). Point mutations of the *p53* gene have been reported in a wide variety of carcinomas. Human NSCLC³ is one of the most common cancers, and lung tumors frequently have *p53* mutations (6). These observations led us to evaluate the antitumor properties of the wt-*p53* gene in a three-dimensional lung cancer spheroid model.

Received 6/11/93; accepted 8/4/93.

The costs of publication of this article were defrayed in part by the payment of page charges. This article must therefore be hereby marked *advertisement* in accordance with 18 U.S.C. Section 1734 solely to indicate this fact.

¹ Partially supported by grants from the National Cancer Institute and NIH (RO1 CA45187) (J. A. R.) and (RO1 CA45225) (E. A. G.), by National Cancer Institute of Training Grant (CA09611-01) (J. A. R.), by gifts to the Division of Surgery from Tenneco and Exxon for the Core Lab Facility, by the M. D. Anderson Cancer Center Core Grant (NCI CA16672), and by a grant from the Mathers Foundation (J. A. R.).

² To whom requests for reprints should be addressed.

³ The abbreviations used are: NSCLC, non-small cell lung cancer; TGF, transforming growth factor; CFU, colony-forming units; PCR, polymerase chain reaction; TdT, terminal deoxynucleotidyl transferase; mut-*p53*, mutated *p53*; wt-*p53*, wild-type *p53*; cDNA, complementary DNA.

The results presented here demonstrate that the wt-*p53* retroviral vector can penetrate into three-dimensional spheroids of the H322a NSCLC cell line and induce programmed cell death of tumor cells. The multicellular tumor spheroid model used in these experiments exhibits *in vitro* a histological structure similar to that of primary tumors and micrometastases (7).

Materials and Methods

Cells and Culture Conditions. Human NSCLC cell lines H322a, which has mut-*p53* at codon 248, and WT226b, which has wt-*p53*, were routinely propagated in monolayer culture in RPMI 1640 containing 10% fetal calf serum (Sigma Chemical Co., St. Louis, MO). The amphotropic packaging cell line GP+envAm12 (2) was grown in Dulbecco's modified Eagle's medium (GIBCO, Grand Island, NY) with a high glucose content (4.5 g/liter) and supplemented with 10% newborn calf serum.

Growth Factor. Recombinant TGF- α (Biosource International, Wetlake Village, CA) was reconstituted in phosphate-buffered saline.

Spheroid Culture. Single cell suspensions were obtained by trypsinization of monolayer cultures: 5×10^5 cells were seeded in 5 ml of culture medium in 60-mm Petri dishes based-coated with 3 ml of 1% medium agar. After 2 to 4 days, small spheroidal aggregates were selected with a Pasteur pipet and placed in individual wells of a 24-well plate containing a 0.5-ml base of 1% agar and a 1-ml overlay of culture medium with or without TGF- α . The perpendicular diameters of the spheroids were measured by using an inverted microscope. The relative increase in volume was calculated according to the formula:

$$\frac{a^2 \times b}{a_1^2 \times b_1}$$

where *a* and *b* are the smallest and largest diameter of the spheroid, respectively, and *a*₁ and *b*₁ are the diameters on day 1.

Recombinant Retroviruses. The construction of retroviral vectors and the generation of a stable vector-producing cell line have previously been reported (8). Briefly, the 6.6-kilobase *EcoRI/NdeI* fragment containing the β -action promoter and wt-*p53* cDNA was subcloned into the LNSX retroviral vector (1). The 1.6-kilobase *HindIII* fragment containing mut-*p53* cDNA (codon 273; CGT to CAT), a gift from Dr. B. Vogelstein, was also cloned into a LNSX vector. Amphotropic packaging cell line GP+envAm12 was transfected with these recombinant constructs by the calcium phosphate coprecipitation method. The highest-titer virus-producing clones were selected, and the supernatant from these clones was used for further experiments. The titers of the retroviral supernatants were 10^6 CFU/ml for the wt-*p53* and 7×10^5 CFU/ml for mut-*p53* vectors (9). The retroviral supernatants were free of replication-competent virus as assessed by an NIH-3T3 amplification assay capable of detecting five infectious viral particles/ml (2). *p53* mRNA and protein were stably expressed in monolayer culture of NSCLC cell lines 6 months after transduction by these retroviruses (8).

Preparation of Tissue Sections. Spheroids were fixed in 4% freshly prepared paraformaldehyde in phosphate-buffered saline for 30 min at 4°C, soaked in methanol/acetic acid (3:1, v/v), and then embedded in paraffin using standard histological techniques. Paraffin-embedded tissues were cut into 5- μ m sections and used for *in situ* PCR/hybridization study or TdT-mediated dUTP-biotin nick labeling to detect programmed cell death.

Probe Preparation. A 190-base pair fragment of the neomycin-resistant *neo* gene was amplified by PCR using the LNSX vector as a template. Primers were forward: 5'-GAT GGA TTG CAC GCA GGT TC-3'; and 5'-CGC TGC CTC GRC CTG CAG TT-3'. The reaction was run in a DNA Thermal Cycler (Perkin-Elmer Cetus, Norwalk, CT) for 35 cycles under these conditions: denaturation at 92°C for 1 min; annealing at 60°C for 1 min; extension at 72°C for 2 min. The *neo* probe was labeled nonradioactively with digoxigenin (Boehringer Mannheim, Indianapolis, IN) by the random primed reaction technique.

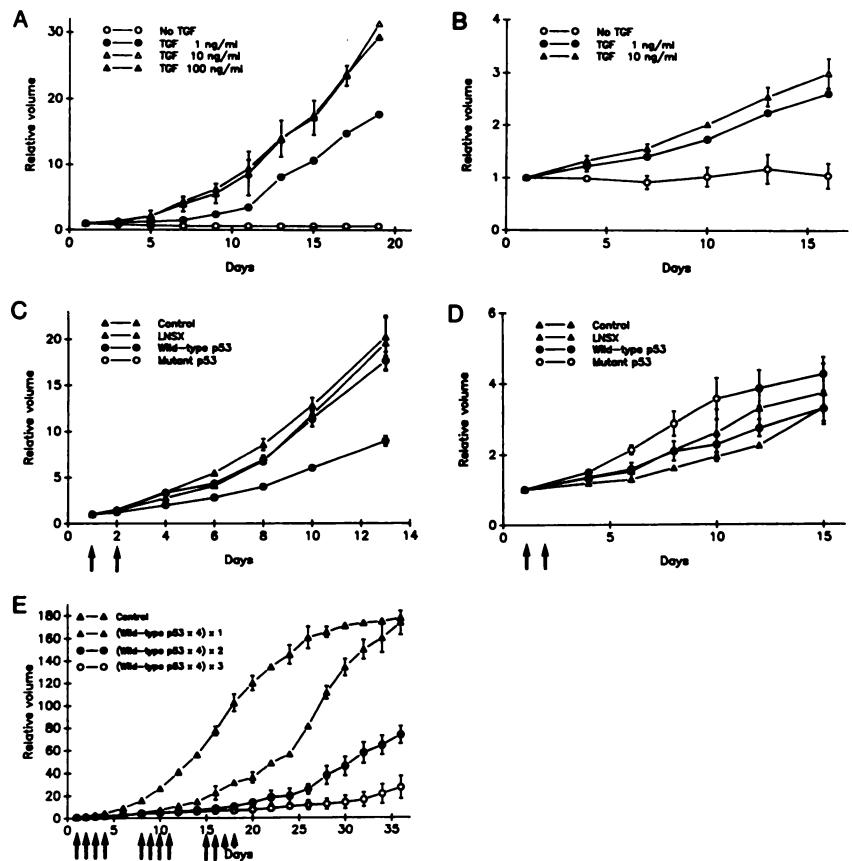
In Situ PCR/Hybridization. Paraffin-embedded sections were deparaffinized in xylene and rehydrated. Tissues were then digested with 10 µg/ml of proteinase K in 50 mM Tris-HCl and 5 mM EDTA (pH 8.0) for 15 min at 37°C. *In situ* PCR was performed with slight modifications of the procedure previously reported (10). After 3 h preincubation with PCR solution containing primers for *neo* at 45°C, the slides were heated to 80°C. Preheated PCR solution with 2% NuSieve GTG agarose (FMC Bioproducts, Rockland, ME) was added to the slides before the coverslips were placed. After sealing with rubber cement, the slides were placed on the heating block of a DNA Thermal Cycler. The PCR reaction was performed for 50 cycles under the following conditions: denaturation at 92°C for 1 min; annealing at 55°C for 2 min; extension at 72°C for 2 min. After removing the coverslips, the slides were fixed in 4% paraformaldehyde at 4°C for 30 min. The slides were dehydrated and prehybridized in a solution containing 50% formamide, 1× Denhardt's solution, 10% dextran sulfate, 0.3 M NaCl, 10 mM Tris-HCl (pH 8.0), 5 mM EDTA, and 100 µg/ml salmon sperm cDNA at 42°C for 4 h. Hybridization was performed in the same solution containing digoxigenin-labeled DNA probe for *neo* at 42°C for 24 h. After hybridization, the slides were blocked with 1% (w/v) blocking reagent in 100 mM Tris-HCl and 150 mM NaCl (pH 7.5) for 30 min and incubated with mouse antidigoxigenin antibody (Boehringer Mannheim) for 1 h at room temperature. After rinsing, the slides were incubated for 2 h with gold-conjugated antimouse immunoglobulin G (IgG) antibody as a secondary antibody followed by silver enhancement (Accurate Chemical & Scientific Corp., Westbury, NY). All sections were counterstained with methylgreen and studied under the light microscope.

Detection of Programmed Cell Death *in Situ*. DNA breaks in nuclei were labeled *in situ* according to the procedure outlined by Gavrieli (11). Briefly, the sections treated with 10 µg/ml proteinase K for 15 min at 37°C were immersed in TdT buffer [30 mM Trizma base (pH 7.2), 140 mM sodium cacodylate, 1 mM cobalt chloride] and incubated with TdT and biotinylated dUTP (Boehringer Mannheim) at 37°C for 1 h. After they were rinsed, the slides were covered with 2% bovine serum albumin for 10 min at room temperature, incubated with extra-avidin peroxidase at 37°C for 30 min, and stained with 3-amino-9-ethylcarbazole for 20 min at 37°C. Finally, tissues were counterstained with hematoxylin.

Results and Discussion

Human NSCLC cell lines H322a and WT226b, which have been previously characterized, have endogenous *mut-p53* and *wt-p53* genes, respectively, and can be grown as spheroids. We previously reported that H322a and WT226b cells have an autocrine growth mechanism mediated by TGF-α and that the addition of exogenous TGF-α increased the formation and growth in soft agar of both cell lines (12). TGF-α stimulated the growth of both H322a and WT226b spheroids in a dose-dependent manner (Fig. 1, A and B). TGF-α was used at a concentration of 10 ng/ml for the stimulation of spheroid growth in subsequent experiments. The effect of *wt-p53* retroviral infection on the growth of H322a and WT226b spheroids was next examined. On day 0, spheroids were placed in a 24-well agar-coated plate. On days 1 and 2, the medium was replaced with retroviral stock [1 ml of LNSX vector and *wt-p53* vector (1×10^6 CFU/ml); 1.4 ml of *mut-p53* vector (7×10^5 CFU/ml)] in the presence of polybrene (10 µg/ml) and TGF-α (10 ng/ml). Fresh medium with 10 ng/ml of TGF-α was added on day 3, following removal of virus-containing medium. Control groups consisted of untreated spheroids or spheroids exposed to the retroviral vector without *p53* or the *mut-p53* retroviral vector.

Fig. 1. Effects of TGF-α on the growth of H322a (A) and WT226b (B) spheroids. Spheroids with a diameter of 200 to 300 µm were cultured in a 24-well plate with a 0.5-ml agar base and 1-ml medium overlay containing various concentrations of TGF-α. The relative volume increase was calculated as described in "Materials and Methods." Points, average of three to six spheroids; bars, SD. Effects of *wt-p53* retroviral infection on the growth of H322a (C) and WT226b (D) spheroids. Spheroids were placed in individual wells on day 0 and infected once daily for 2 days with retroviral stock in the presence of 10 µg/ml polybrene and 10 ng/ml TGF-α. On day 3, the liquid overlay was replaced with fresh medium containing TGF-α (10 ng/ml). The relative volume increase was calculated by measuring perpendicular diameters. E, effects of multiple cycles of *wt-p53* infections on the growth of H322a spheroids. Serial infection with *wt-p53* retroviral stocks for 4 days in the presence of polybrene (10 µg/ml) and TGF-α (10 ng/ml) were repeated weekly up to 3 times. The data are presented as relative volume increase.



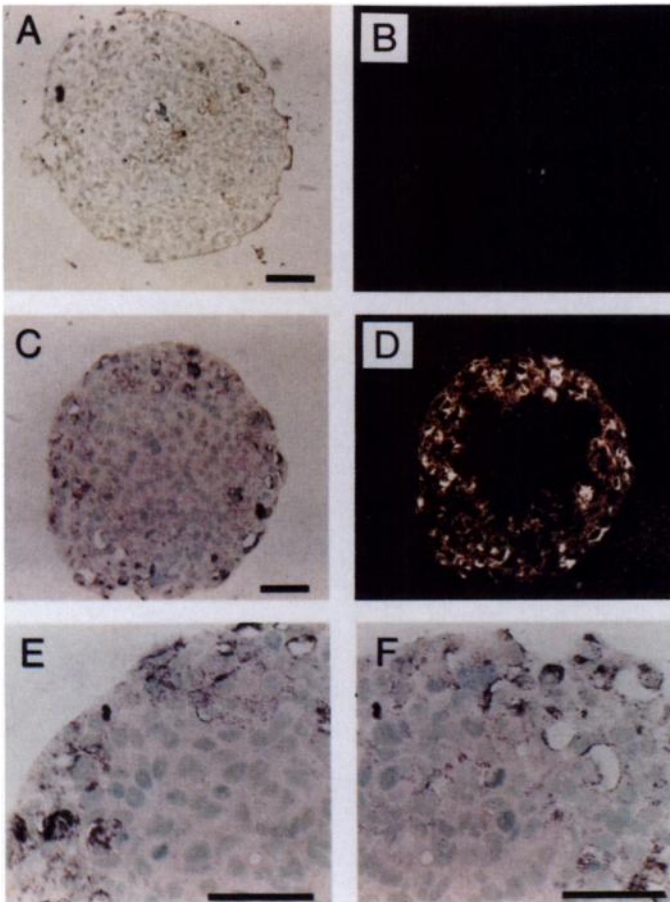


Fig. 2. *In situ* PCR/hybridization of sections of H322a spheroids infected with wt-*p53* retrovirus. H322a spheroids were infected with wt-*p53* retroviral stocks daily from day 1 to 4 as described in the legend to Fig. 1. *In situ* PCR was performed using *neo* primers for 50 cycles. Amplified *neo* gene was hybridized with a 190-base pair digoxigenin-labeled *neo* probe and detected by antidigoxigenin antibody as described in "Materials and Methods." A and B, untreated spheroid controls. C-F, H322a spheroids infected with wt-*p53* (spheroid 1 on day 6 listed in Table 1). B and D, dark field views of A and C. Bars, 100 μ m. Positive signals were detected over the cells as scattered silver grains under the bright field. A dark-field illumination demonstrated signals as bright dots. Proviral sequences were not detected without PCR amplification.

Table 1 Penetration of retroviral vector containing the wt-*p53* gene into H322a spheroids

Days ^a	Diameters ^b (μ m)	Depth ^c (μ m)	No. of cell layers ^c
2	340 \times 320	16.3 \pm 12.7	1.00 \pm 0.7
4	440 \times 380	35.0 \pm 15.8	1.75 \pm 1.09
6	Spheroid 1	570 \times 530	96.3 \pm 26.4
	Spheroid 2	500 \times 480	74.3 \pm 20.6
	Spheroid 3	620 \times 550	86.3 \pm 23.4

^a Days after the initiation of viral infection. H322a spheroids were exposed to the retroviral stock for 4 days as described in the legend to Fig. 1.

^b Perpendicular long diameter \times short diameter.

^c Depth from the surface and the number of cell layers penetrated by retrovirus were measured with a light microscope at 45° intervals in spheroid sections. Eight measurements were performed and the mean \pm SD was calculated.

Exposure to the wt-*p53* vector suppressed TGF- α -dependent growth of H322a spheroids but had no effect on the growth of WT226b spheroids (Fig. 1, C and D). These findings are consistent with our previous results obtained by using monolayer culture of NSCLC cell lines transduced with wt-*p53* (8). Multiple cycles of infection were more effective at suppressing multicellular tumor spheroid growth than a single cycle (Fig. 1E).

The dynamics of retrovirus-mediated *in vivo* gene transduction have been studied by using the *Escherichia coli lacZ* (β -galactosidase) gene

as a reporter gene (13). Clonogenic assays of tumor cells regrown from virus-injected mice were also used to evaluate the transduction efficacy of retroviral genes into a tumor mass (14). They showed that greater than 95% cells were infected by retrovirus *in vitro*. However, data about time-related virus penetration into three-dimensional tumor structures and *in situ* viral localization have not been previously reported. Therefore, we studied the localization of the wt-*p53* vector in H322a spheroids by *in situ* hybridization. Our studies used the neomycin resistance (*neo*) gene expressed by the vector as a target sequence because it is not possible to distinguish transduced wt-*p53* gene from endogenous mut-*p53* gene expressed in H322a cells by this technique. An *in situ* PCR method was used to amplify a single copy of integrated DNA (10). After 2 days of viral exposure, the wt-*p53* retroviral vector sequences were located only at the spheroid surface; after 6 days, however, the *neo* gene was detected in the deeper areas of the spheroids (Fig. 2; Table 1), demonstrating that retroviral vectors can penetrate into solid tumors.

The retroviral vectors were not integrated into H358 (*p53* deleted) spheroids (data not shown). These spheroids showed no growth in response to TGF- α suggesting that active tumor cells proliferation is an important requirement for retroviral integration. For some types of applications, this characteristic is considered one of the disadvantages of the retroviral vectors. For example, in cystic fibrosis, gene transduction is inhibited by the low mitotic activity of airway epithelial cells (15). However, since malignant tumor cells are usually associated with an increase in synthesis of replicative DNA, the dependence of retroviral transduction on proliferation may be useful for selective gene targeting in cancer therapy.

Morphological studies demonstrated that H322a spheroids displayed vacuole formation in areas close to the spheroid surface 6 days after the initiation of exposure to the wt-*p53* retrovirus exposure (Fig. 3). The untreated control spheroids, those transduced with the LNSX vector alone, and those transduced with mut-*p53* showed no surface vacuole formation during this time period. Histological study with hematoxylin and eosin staining showed dead cells in and around

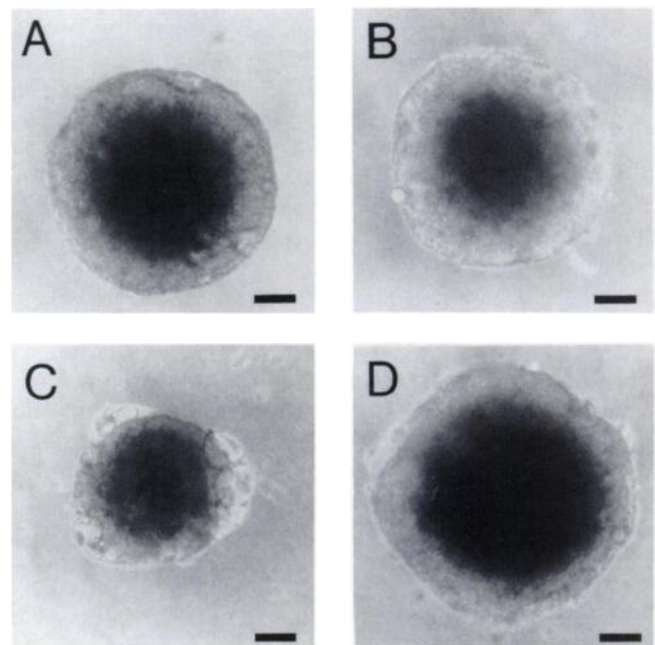


Fig. 3. Gross morphology of H322a spheroids on day 6 after the beginning of a 4-day infection period. H322a spheroids were exposed to retroviral stocks as described in the legend to Fig. 1 for 4 days. A, untreated spheroids; spheroids infected with the LNSX vector only (B); the LNSX/wt-*p53* vector (C); or the LNSX/mut-*p53* (D). Bars, 100 μ m.

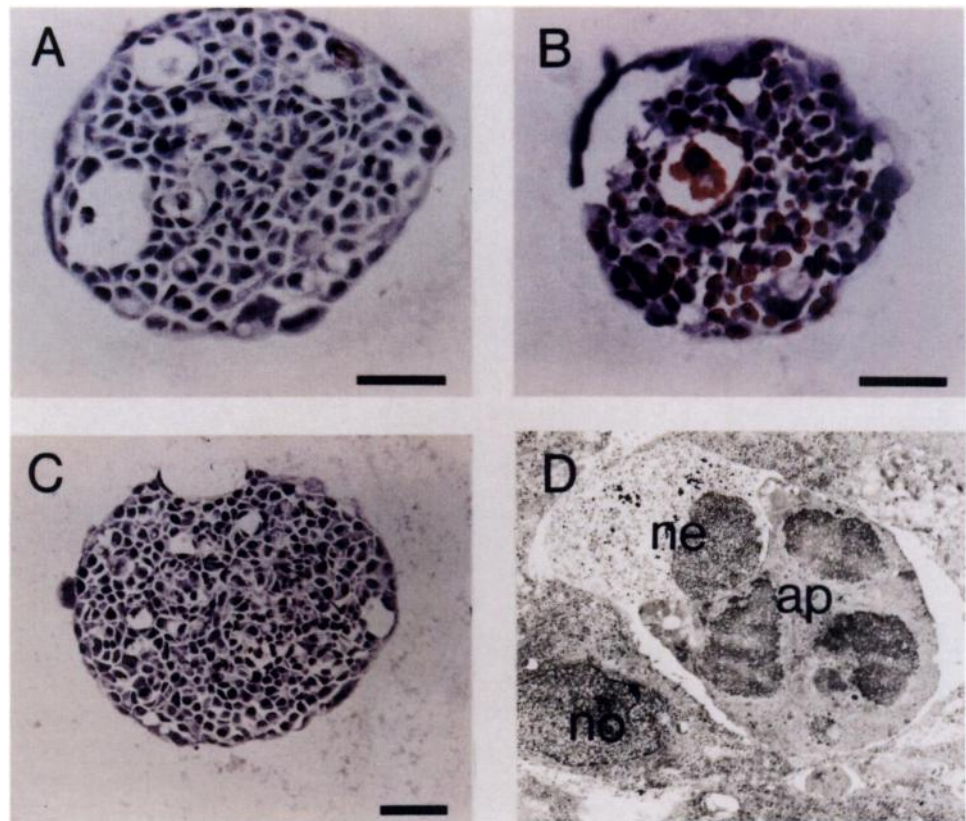


Fig. 4. *In situ* detection of programmed cell death by TdT-mediated dUTP-biotin nick end labeling on H322a spheroids treated with the wt-*p53* retroviral vector. H322a spheroids were infected with retroviral stocks for 4 days as described in the legend to Fig. 1. A, untreated spheroids; B, spheroids infected with the wt-*p53* vector; C, spheroids infected with mut-*p53* vector. All spheroids are shown on day 6. Bars, 100 μ m. D, electron micrograph of spheroid infected with wt-*p53* LNSX vector (on day 6). H322a spheroids were fixed in 0.1 M sodium cacodylate buffer with 3% glutaraldehyde and 2% paraformaldehyde for 1 h. \times 5400. *ap*, apoptotic cell; *no*, normal cell; *ne*, necrotic cell.

vacuoles (data not shown). As shown in Fig. 2, the *neo* marker (indicative of retroviral transduction) was detected around vacuoles, indicating that retroviral transduction was associated with cell death.

Programmed cell death, also known as apoptosis, shows a characteristic pattern of DNA fragmentation resulting from cleavage of nuclear DNA and is considered to be a selective process of physiological cell deletion. It has recently been reported that the wt-*p53* gene is involved in mediating programmed cell death of some types of tumor cells (16, 17). Apoptotic cells can be detected histologically, but we used a recently developed, more sensitive *in situ* method of detecting the DNA fragmentation found in morphologically intact cells that are in the process of programmed cell death. This method allowed us to identify the nature of the cell death induced by wt-*p53* transduction. Specific *in situ* labeling of DNA fragmentation with biotin-labeled dUTP (11) demonstrated that the wt-*p53* transduction induced apoptosis in H322a cells and that these apoptotic cells were stained throughout the sections of H322a spheroids close to the surface, where retrovirus penetration was detected, 6 days after the beginning of infections (Fig. 4, A-C). It has been reported that the wt-*p53*-induced cell death and cell-cycle arrest in the G₁ phase are separate functions (18) and that wt-*p53* can induce apoptosis as early as 4 h after its expression (17). Although a retroviral system needs time to be integrated and to express the introduced gene, the inhibition of growth of H322a spheroids and surface blebbing on day 6 were mediated by the induction of programmed cell death. Transmission electron microscopy shows cells that display typical apoptotic features, including clumping chromatin, swollen nucleolus, and condensed mitochondria (Fig. 4D).

We previously reported the ability of a retroviral antisense *K-ras* construct to prevent the growth of established orthotopic human lung cancer in *nu/nu* mice (4). Thus, regional administration of retroviral constructs with antioncogene activity can mediate a therapeutic effect. This study provides additional support for this concept by showing

that retroviruses can penetrate into solid tumor masses. It also suggests that retroviral vectors expressing a wild-type tumor suppressor gene can prevent the growth of tumor masses. To the best of our knowledge, this is the first report showing the ability of retroviruses to extensively penetrate into three-dimensional tumor cell masses and to mediate antitumor effects including reduction in tumor cell proliferation and apoptosis of tumor cells within these cell aggregates. Thus, retroviral vectors are capable of penetrating multiple cell layers and mediating potentially therapeutic effects. It is conceivable that regional administration of viral supernatants could be used therapeutically in established tumors and to correct genetic abnormalities described in premalignant lesions of the upper aerodigestive tract and gastrointestinal mucosa (19, 20).

Acknowledgments

We thank Dr. B. Vogelstein (The Johns Hopkins University Oncology Center) for mut-*p53* cDNA and C. Torrence for assistance in preparing the manuscript.

References

1. Miller, A. D., and Rosman, G. J. Improved retroviral vectors for gene transfer and expression. *BioTechniques*, 7: 980-990, 1989.
2. Markowitz, D., Goff, S., and Bank, A. Construction and use of a safe and efficient amphotropic packaging cell line. *Virology*, 167: 400-406, 1988.
3. Gansbacher, B., Daniels, B., Zier, K., Cronin, K., Bannerji, R., and Gilboa, E. Interleukin-2 gene transfer abrogates tumorigenicity and induces protective immunity. *J. Exp. Med.*, 172: 1217-1224, 1990.
4. Georges, R. N., Mukhopadhyay, T., Zhang, Y. J., Yen, N., and Roth, J. A. Prevention of orthotopic human lung cancer growth by intratracheal instillation of a retroviral antisense *K-ras* construct. *Cancer Res.*, 53: 1743-1746, 1993.
5. Lane, D. P. Cancer: *p53*, guardian of the genome. *Nature (Lond.)*, 358: 15-16, 1992.
6. Takahashi, T., Nau, M. M., Chiba, I., Birrer, M. J., Rosenberg, R. K., Vinocour, M., Levitt, M., Pass, H., Gazdar, A. F., and Minna, J. D. *p53*: a frequent target for genetic abnormalities in lung cancer. *Science (Washington DC)*, 246: 491-494, 1989.
7. Schwachofer, J. H. M. Multicellular tumor spheroids in radiotherapy research. *Anti-*

- cancer Res., 10: 963-970, 1990.
8. Cai, D. W., Mukhopadhyay, T., Liu, T., Fujiwara, T., and Roth, J. A. Stable expression of the wild-type *p53* gene in human lung cancer cells after retrovirus-mediated gene transfer. *Hum. Gene Ther.*, 4: 617-624, 1993.
 9. Palmer, T. D., Hock, R. A., Osborne, W. R. A., and Miller, A. D. Efficient retrovirus-mediated transfer and expression of a human adenosine deaminase gene in diploid skin fibroblasts from an adenosine deaminase-deficient human. *Proc. Natl. Acad. Sci. USA*, 84: 1055-1059, 1987.
 10. Chiu, K.-P., Cohen, S. H., Morris, D. W., and Jordan, G. W. Intracellular amplification of proviral DNA in tissue sections using polymerase chain reaction. *J. Histochem. Cytochem.*, 40: 333-341, 1992.
 11. Gavrieli, Y., Sherman, Y., and Ben-Sasson, S. A. Identification of programmed cell death *in situ* via specific labelling of nuclear DNA fragmentation. *J. Cell Biol.*, 119: 493-501, 1992.
 12. Putnam, E. A., Yen, N., Gallick, G. E., Steck, P. A., Fang, K., Akpakip, B., Gazdar, A. F., and Roth, J. A. Autocrine growth stimulation by transforming growth factor α in human non-small cell lung cancer. *Surg. Oncol.*, 1: 49-60, 1992.
 13. Ram, Z., Culver, K. W., Walbridge, S., Blaese, R. M., and Oldfield, E. H. *In situ* retroviral-mediated gene transfer for the treatment of brain tumors in rats. *Cancer Res.*, 53: 83-88, 1993.
 14. Culver, K. W., Ram, Z., Wallbridge, S., Ishii, H., Oldfield, E. H., and Blaese, R. M. *In vivo* gene transfer with retroviral vector-producer cells for treatment of experimental brain tumors. *Science (Washington DC)*, 256: 1550-1552, 1992.
 15. Stanley, C., Rosenberg, M. B., and Friedman, T. Gene transfer into rat epithelial cells using retroviral vectors. *Somatic Cell Mol. Genet.*, 17: 185-190, 1991.
 16. Yonish-Rouach, E., Resnitzky, D., Rotem, J., Sachs, L., Kimchi, A., and Oren, M. Wild-type *p53* induces apoptosis of myeloid leukemic cells that is inhibited by interleukin-6. *Nature (Lond.)*, 352: 345-347, 1991.
 17. Shaw, P., Bovey, R., Tardy, S., Sahli, R., Sordat, B., and Costa, J. Induction of apoptosis by wild-type *p53* in a human colon tumor-derived cell line. *Proc. Natl. Acad. Sci. USA*, 89: 4495-4499, 1992.
 18. Ryan, J. J., Danish, R., Gottlieb, C. A., and Clarke, M. F. Cell cycle analysis of *p53*-induced cell death in murine erythroleukemia cells. *Mol. Cell. Biol.*, 12: 711-719, 1993.
 19. Sozzi, G., Miozzo, M., Donghi, R., Pilotti, S., Cariani, C. T., Pastorino, U., Dellaporta, G., and Pierotti, M. A. Deletions of 17p and *p53* mutations in preneoplastic lesions of the lung. *Cancer Res.*, 52: 6079-6082, 1992.
 20. Casson, A. G., Mukhopadhyay, T., Cleary, K. R., Ro, J. Y., Levin, B., and Roth, J. A. *p53* gene mutations in Barrett's epithelium and esophageal cancer. *Cancer Res.*, 51: 4495-4499, 1991.

Cancer Research

The Journal of Cancer Research (1916–1930) | The American Journal of Cancer (1931–1940)

A Retroviral Wild-type *p53* Expression Vector Penetrates Human Lung Cancer Spheroids and Inhibits Growth by Inducing Apoptosis

Toshiyoshi Fujiwara, Elizabeth A. Grimm, Tapas Mukhopadhyay, et al.

Cancer Res 1993;53:4129-4133.

Updated version Access the most recent version of this article at:
<http://cancerres.aacrjournals.org/content/53/18/4129>

E-mail alerts [Sign up to receive free email-alerts](#) related to this article or journal.

Reprints and Subscriptions To order reprints of this article or to subscribe to the journal, contact the AACR Publications Department at pubs@aacr.org.

Permissions To request permission to re-use all or part of this article, use this link <http://cancerres.aacrjournals.org/content/53/18/4129>. Click on "Request Permissions" which will take you to the Copyright Clearance Center's (CCC) Rightslink site.